# Code Shift Keying
## Prospects for Improving GNSS Signal Designs



**BPSK Modulation**

Bit '1' | Bit '0' | Bit '1' | Bit '1' | Bit '0'

Bits '0000' | Bits '1101' | Bits '0011' | Bits '1000' | Bits '1010'
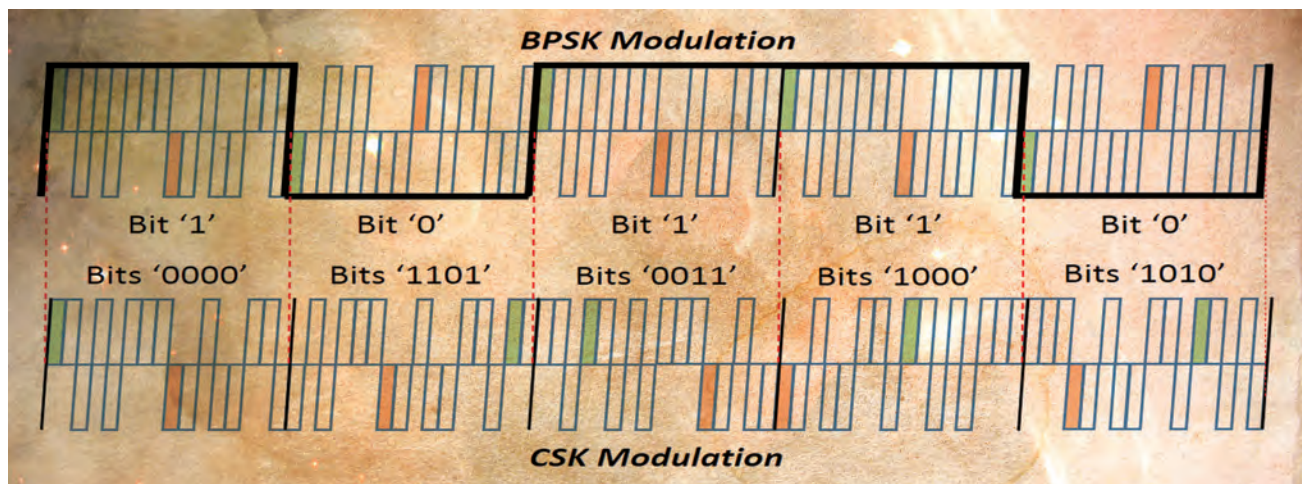
**CSK Modulation**

This article presents the code shift keying (CSK) modulation principle and highlights some of its specific features related to demodulation performance. CSK behaves like a M–ary signaling technology and presents interesting capabilities and features to solve some of the GNSS industry's current dilemmas. CSK provides distinctive demodulation properties but does not outperform BPSK implementation with equivalent bit rate and message time duration for the cases presented here. However, achieving additional improvement of the CSK modulation is still expected; for instance, optimizing error correction codes for CSK may reverse this trend.

**AXEL GARCIA-PEÑA**
ÉCOLE NATIONALE DE L'AVIATION CIVILE (ENAC)

**MARION AUBAULT-ROUDIER, LIONEL RIES**
CNES, THE FRENCH SPACE AGENCY

**MARIE-LAURE BOUCHERET, CHARLY POULLIAT**
NATIONAL POLYTECHNIC INSTITUTE OF TOULOUSE (ENSEEIHT)

**OLIVIER JULIEN**
ENAC

The constant growth and evolution of the positioning, navigation, and timing (PNT) market generate demands for more and more added-value applications and services relying on GNSS signals, with expectations for improved accuracy and availability. Some services may also rely on added-value content other than navigation messages, for example, higher data volume with less latency, such as the data carried by satellite-based augmentation system (SBAS) services and the Galileo Commercial Service.

Among the many drivers that could be considered for possible future GNSS signals, those addressing the data component (higher rate, improved availability, and so forth) may be of particular interest. Although these drivers signifi-

cantly affect the design and performance of GNSS signals, thus calling for specific attention, their implementation may not necessarily require innovative technical solutions.

Nevertheless, alternative or innovative approaches may conceivably provide better or different trade-offs of the various drivers, requirements, and constraints, than the existing ones. Novel approaches should therefore be explored, and their adaptation to GNSS assessed, either to gain understanding and raise technical maturity — the Technology Readiness Level or TRL — so that these approaches become suitable candidates for future design, or to confirm that current solutions still provide the most appropriate trade-off.

One such example could be the analysis of implementations to transport data bits on GNSS signals. The classical approach consists of applying the equivalent bit or encoded symbol value sign (+1 or -1) directly onto the pseudo-random noise (PRN) waveform. Traditionally, this technique has been identified with BPSK or BPSK modulation, in reference to the non-return-to-zero BPSK (NRZ-BPSK) scheme, although this technique could also be applied to xBOC (binary offset carrier ) signals: BOC, alternative BOC (ALTBOC), multiplexed BOC, and so on.

*Code shift keying* (CSK) or *code cyclic shift keying* (CCSK) is an alternative technique to the aforementioned BPSK technique. Previously used in some code division multiple access (CDMA) communication standards, CSK modulation has lately been incorporated in the Quasi-Zenith Satellite System (QZSS) L-band Experimental (LEX). LEX has a higher bit rate than the other components of QZSS and, generally speaking, other GNSS signals: 2,000 encoded bits per seconds.

This article relates ongoing research on the CSK modulation as an alternative to BPSK for future GNSS signals, allowing increased data rates, along with the use of non-coherent demodulation methods. We first introduce the CSK principles and distinctive features, followed by presentation of the associated mathematical models. Later, we report some performance assessment results, both in terms of effects on a GNSS receiver and in terms of demodulation performance. Finally, as work is still ongoing, we identify future efforts that could take advantage of CSK modulation in urban environments.

## CSK Modulation: A Differentiator for Future GNSS Signals

The CSK modulation was specially designed to increase the transmission rate of a band-limited spread spectrum signal without affecting the PRN code structure. The main idea of a CSK modulation consists in increasing the number of different PRN codes transmitted on the data component.

The new PRN codes are obtained by circularly shifting a fundamental PRN code (see **Figure 1**). Therefore, since each PRN code represents one symbol, CSK modulation increases the number of available symbols with respect to BPSK modulation.

Increasing the number of symbols of the modulation alphabet implies that more bits can be mapped by each symbol (four symbols can transmit two bits, eight symbols corresponds to 3 bits, and so on). So, if each PRN code period is equal to the data symbol duration, the bit transmission rate of a CSK modulation compared to a BPSK modulation

(where one PRN code spans one symbol) is increased proportionally to the number of bits mapped by a CSK symbol. The demodulator only needs to identify which PRN code was transmitted to estimate the corresponding symbol and set of bits.

Among all possible drivers for future evolutions of the GNSS signals, we identified at least three distinctive features that relate to the information content or messages.

A first driver could be an increase of the bit rate in order to accommodate new services and/or additional data to enhance signal integrity, robustness, and so forth or added-value information: high-accuracy satellite clock and ephemeris data (CED), integrity information, acquisition-aiding data, authentication, etc.

The related data can be obtained by using an additional telecommunication link (ground or space), as in precise point positioning or assisted-GNSS. As this implies a dependence on telecommunication networks and a higher receiver complexity, it is therefore not suitable for users unwilling or unable to depend on systems external to GNSS (such as civil aviation, "white areas" with undeveloped communications infrastructure, high latitude areas where GEO satellites are unavailable, and so on). Thus, the ability to broadcast data other than navigation CED messages seems to remain relevant for the future of GNSS signals.

Second, allocation of different data rates to distinct parts of the GNSS signal's messages may attract some interest in the future. For example, this may be useful to sustain different channel codes, diversity, or redundancy, different data latency, and so on, or to

manage different services having distinct targeted users, requirements, and relevance.

Third, signal availability in urban environments remains a challenge for current and future GNSS messages/signal designs. Signal data availability is defined as the amount of time when the data can be successfully delivered with respect to the total amount of time. In urban areas, the received signal is severely impacted by obstacles that generate fast and significant variations of the received signal's phase and amplitude, which are detrimental to both synchronization and demodulation.

One solution to increase the signal availability, which would benefit from a higher data rate, could be to improve code correction schemes. Another solution would be to transmit data at a very high rate in order to best use favorable reception conditions: the user benefits from the time slots when the signal is not obstructed (e.g., on wide avenues, at street crossings). The rapid variations and the strong impact on the urban propagation channel result in a large number of phase locked loop (PLL) losses of lock during which messages cannot be demodulated. A very interesting and complementary approach to improve data availability would be for the receiver to rely on equalization techniques combined with non-coherent demodulation schemes.

Together, these three drivers may call for GNSS signal designs with higher data rates than current ones, with potentially variable data rates, combined with robust demodulation capabilities in the absence of good carrier phase estimation. CSK represents a potential implementation to efficiently meet such stringent requirements.
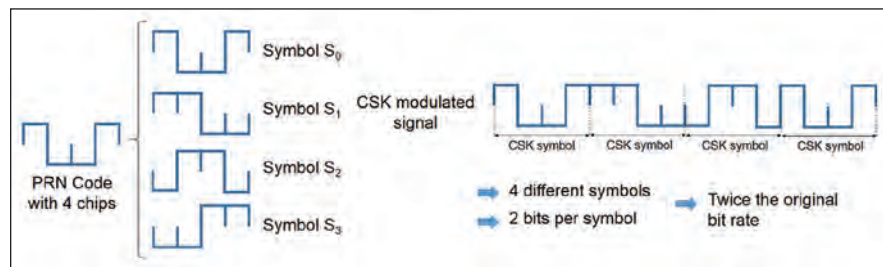


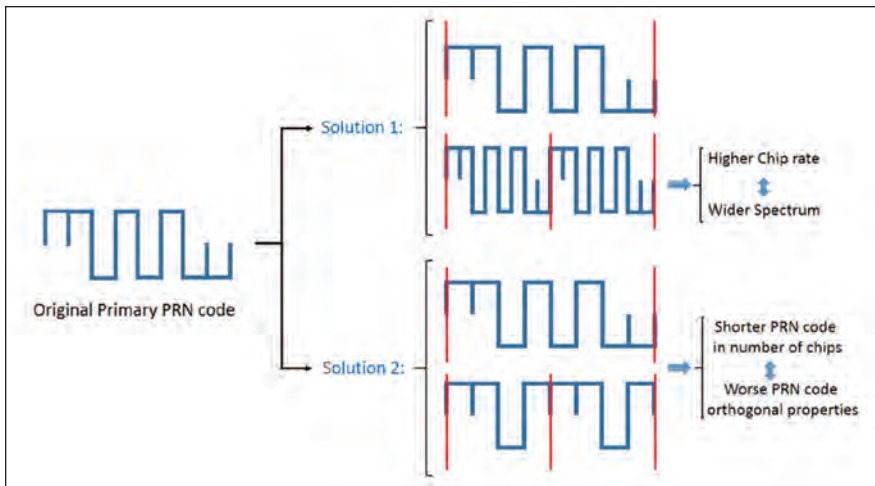**FIGURE 1** CSK symbol generation and CSK modulated signal

**FIGURE 2** Two solutions to increase the data bit rate of a BPSK modulated signal
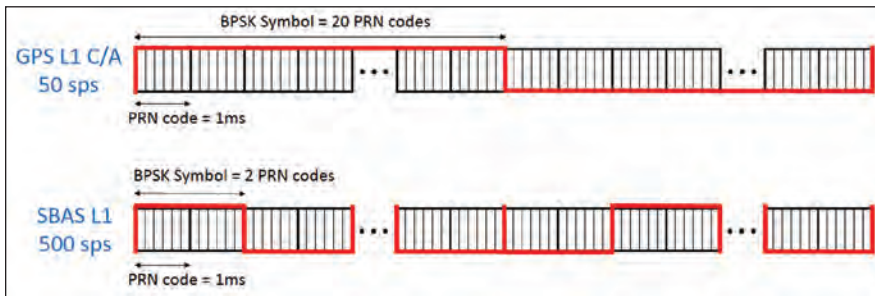


**FIGURE 3** Different symbol rates for GPS L1 C/A and SBAS L1 despite having the same primary PRN code structure

Using classical direct-sequence spread spectrum (DS-SS) and a BPSK modulation, a faster data rate could lead to two suboptimal solutions: either to increase the PRN code chip rate, resulting in a wider spectrum, or to decrease the PRN code length, resulting in a loss of PRN code isolation and orthogonal properties (see **Figure 2**).

In order to avoid changing the primary PRN code properties while increasing or changing the signal data rate, the traditional solution has been to decrease the number of primary PRN codes spanning a BPSK symbol, e.g., GPS L1 C/A versus SBAS C/A as seen in **Figure 3**, or Galileo E5b versus E5a messages. This method is limited to one PRN code per BPSK symbol and is restrained by the allocated band (chip rate) and interference levels (PRN code isolation properties), and is thus theoretically suboptimal as compared to CSK.

CSK modulation is able to sustain a diversity of bit rates while keeping the same symbol rate (and thus, the same PRN properties), with no effect on the receiver's CSK demodulator and the signal cross-correlation performances.

Also, the BPSK modulation may suffer significant losses when facing a degraded environment, such as urban propagation channels, due to its sensitivity to the accuracy of carrier phase estimation. However, when facing such environments, CSK is expected to provide a high potential for increasing signal availability thanks to its principle of mapping information data bits in the time domain (PRN shift) rather than in the amplitude/phase domain.

## CSK Fundamentals

The CSK modulation technique is a DS–SS signaling method that overcomes the spreading gain versus data rate limitations (See the paper by A. Y.-C. Wong *et alia* in Additional Resources near the end of this article). As discussed in the article by G. M. Dillard *et alia*, the CSK is a form of orthogonal *M*-ary signaling over a communication channel because orthogonal symbols are used in order to transmit $U = \log_2(M)$ bits. The special characteristic of the CSK modulation with respect to the typical orthogonal *M*-ary modulation is that each symbol (representing a set of input bits) is obtained from a different circular cyclic code phase shift of a single fundamental PRN sequence. Moreover, each circular cyclic code phase shift is made by an integer number of chips and is assumed to be a full period version of the fundamental sequence.

**Mathematical Models of CSK Symbol and Signal.** The CSK symbol mathematical model depends on the number of possible shifts of the fundamental PRN code, *M*, and on the number of identical shifted PRN codes that constitute a CSK symbol, *N*. The number of different circular shifts of the fundamental PRN code that are required to transmit *U* bits per CSK symbol is equal to *M*, where $M = 2^U$.

The CSK fundamental code is called $c_d(t)$ and has a period length equal to $T_{PRN}$ which spans over *C* chips. *C* is not necessarily equal to *M* and the chip interval is equal to $T_c$. From this fundamental code, $c_d(t)$, the modulator generates the *M* circular PRN code shifts, referred to as $c_0(t)$ to $c_{M-1}(t)$. A mathematical expression of a generic circular PRN code shift is shown below:

$$c_x(t) = c_d(mod[t - m_x T_c, C \cdot T_c]) \quad \text{(1)}$$
$$c_x[m] = c_d(mod[m - m_x, C])$$
$$x = 0 \dots M - 1$$

$$c_x(t) = \sum_{m=0}^{C-1} c_x[m] \cdot rect\left(\frac{t - mT_c}{T_c}\right) \quad \text{(2)}$$

where $m_x$ is the integer number representing the code shift of the $x^{\text{th}}$ symbol and $mod(x,y)$ represents the modulus operation of *y* over *x*. The CSK symbol mathematical model, $s_x(t)$, is thus obtained by repeating *N* times the circular shifted PRN code shift representing the set of bits that are transmitted:

$$s_x(t) = \sum_{n=0}^{N-1} c_x(t - nT_{PRN}) \quad \text{(3)}$$

The CSK symbol length, $T_s$, is thus defined as $T_s = NT_{PRN}$. The equivalent low-pass CSK-modulated signal at the emitter's antenna output is simply modeled as:

$$s_l(t) = \sqrt{2P_{trans}} \sum_{i=-\infty}^{+\infty} s_{x[i]}(t - iT_s) \quad \text{(4)}$$

where $P_{trans}$ is the transmitted CSK signal power, and $x[i] \in [0, M-1]$ indicates the transmitted CSK symbol at instant $i$. The equivalent low-pass received signal at the receiver RF block output, $v_l(t)$, can be modeled when assuming the transmission of a CSK signal through a narrowband non-frequency selective channel (see the book by J. G. Proakis *et alia*) as:

$$v_l(t) = \sqrt{2P} \cdot c(t) \cdot s_l(t) + n(t) \quad (5)$$
$$c(t) = a(t)e^{j\varphi(t)}$$

where $P$ is the received signal power (without taking into account the propagation channel influence), $c(t)$ is the complex envelope introduced by the propagation channel, $\varphi(t)$ is the instantaneous carrier phase introduced by the propagation channel, $a(t)$ is the amplitude introduced by the propagation channel, and $n(t)$ is the equivalent low-pass AWG noise with power equal to $\sigma^2$.

From now on in this article, a CSK configuration $CSK(U,N)$ is defined as a CSK modulated signal where each symbol maps $U$ bits and $N$ consecutive and identical PRN codes constitute a symbol (see **Figure 4**). The main idea driving the use of consecutive PRN codes in order to constitute a CSK symbol is the possibility of obtaining a relatively small bit rate increase value by using a CSK symbol mapping a large number of bits, $U$.

According to this nomenclature, the bit rate increase of a CSK modulation with respect to a BPSK modulation where each BPSK symbol spans one fundamental PRN code is equal to:
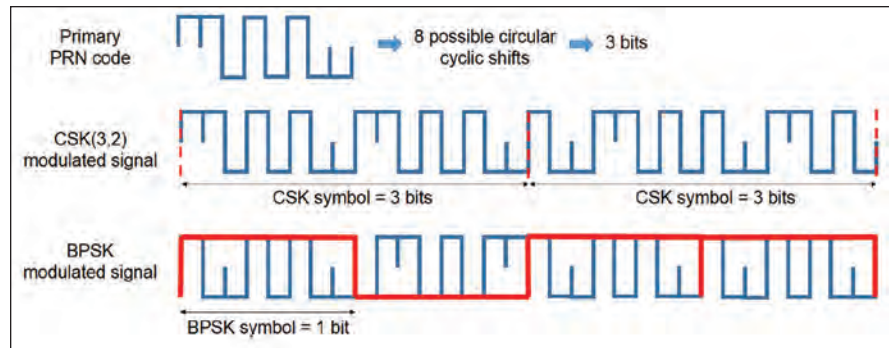
*Bit rate increase = U/N* (6)



**FIGURE 4** *CSK(U, N)* configuration example

The foregoing example illustrates the main differentiator of the CSK. Indeed, while having the same PRN code properties (and performances) over the same period of time, the CSK (3,2) signal transmits six bits whereas the BPSK only transmits four bits.

## Mathematical Model of CSK Demodulator Output

The principle of an orthogonal $M$-ary modulation demodulator consists, first, in applying a matched filter for each symbol of the alphabet and, second, in choosing the symbol identified by the largest matched filter output as the transmitted symbol. Therefore, the CSK demodulator consists of two banks of matched filters, one in in-phase and another in quadrature-phase for each possible PRN code shift (see **Figure 5**).

Assuming a perfect code delay synchronization, a perfect orthogonality between any two PRN code shifts, and that the symbol $x$ was transmitted at instant $i$, the in-phase and quadrature-phase outputs of the $k^{th}$ matched filter at instant $i$, $y_k^{I,i}$, can be modeled as:

$$y_k^{I,i} = \begin{cases} C_i^I + n_k^{I,i} & x = k \\ n_k^{I,i} & x \neq k \end{cases} \quad y_k^{Q,i} = \begin{cases} C_i^Q + n_k^{Q,i} & x=k \\ n_k^{Q,i} & x \neq k \end{cases} \quad (7)$$
$$k = 0 \ldots M-1$$

$$C_i^I = \text{Re}\left[\frac{1}{T_s}\int_{(i-1)T_s}^{iT_s} a(t)e^{j\varepsilon_\varphi(t)}dt\right] \quad (8)$$

$$C_i^Q = \text{Im}\left[\frac{1}{T_s}\int_{(i-1)T_s}^{iT_s} a(t)e^{j\varepsilon_\varphi(t)}dt\right]$$

$$\varepsilon_\varphi(t) = \varphi(t) - \hat{\varphi}(t)$$

where $\hat{\varphi}(t)$ is the carrier phase estimation, $n_k^{I,i}$ and $n_k^{Q,i}$ are independent (due to PRN code shift orthogonality) narrowband Gaussian noises with power equal to $\sigma^2 = (R_s \cdot N_0)/(2P)$, and $R_s$ is the CSK symbol rate ($R_s = 1/T_s$). From Equation (7), it can be observed that due to PRN code orthogonal properties, only the matched filter output of the transmitted symbol has a useful term, $C_i^I$ or $C_i^Q$, whereas the other matched filters outputs only contain noise.

Vector $Y^{I,i}$ represents the in-phase outputs of the matched filters and for a coherent demodulation process, vector $Y^{I,i}$ suffices to demodulate the data (J. G. Proakis *et alia*) by choosing the symbol
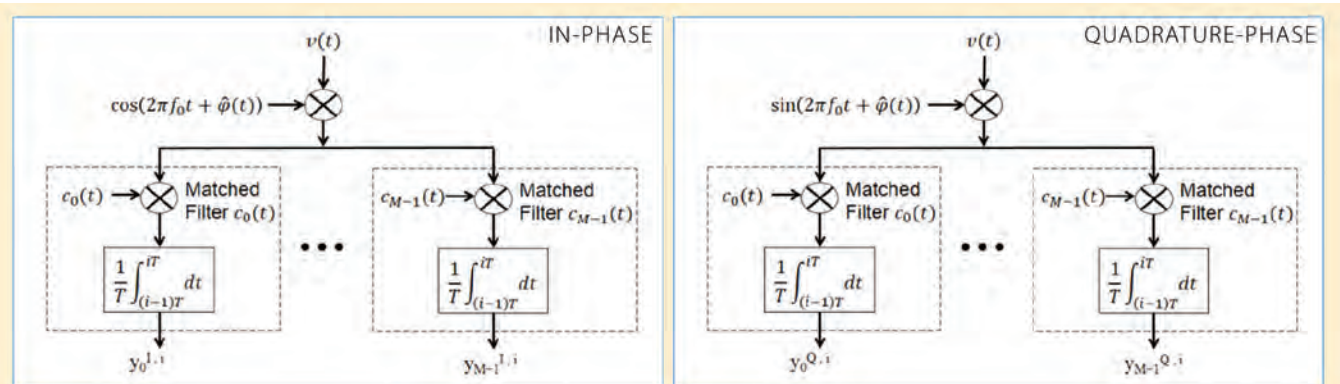


**FIGURE 5** CSK demodulator: a bank of matched filters

identified by the largest matched filter output as the estimated symbol.

$$Y^{l,i} = \left[ y_0^{l,i}, y_1^{l,i}, \ldots, y_k^{l,i}, \ldots, y_{M-1}^{l,i} \right] \qquad (9)$$

The sensitivity of the coherent demodulator to phase estimation errors, shown by Equation (8), may be overcome thanks to a non-coherent demodulation using a new vector, with components $|y_k^i|$ (noiseless expression):

$$|y_k^i| = \sqrt{\left(y_k^{l,i}\right)^2 + \left(y_k^{Q,i}\right)^2} = \frac{1}{T_s} \sqrt{\left| \int_{(i-1)T_s}^{iT_s} a(t) e^{j\varepsilon_\varphi(t)} dt \right|^2} \quad k=0,\ldots,M-1 \quad (10)$$

This non-coherent demodulation still requires good frequency Doppler estimation, with errors typically lower than $\frac{1}{4T_s}$ to constrain power losses below one decibel.

Finally, as each CSK symbol is a circular shift of the fundamental PRN sequence, an efficient demodulator implementation would rely on the computation of the correlation function in the frequency domain using discrete Fourier transform (DFT) — or Fast Fourier transform (FFT) and inverse discrete Fourier transform (IDFT) or IFFT — because this type of demodulator conducts a smaller number of operations than a correlator-based demodulator(A. Garcia-Pena *et alia*, 2010). **Figure 6** shows the scheme of the DFT-based CSK demodulator in which the demodulator could be improved by replacing the DFT by an FFT. (*v[k]* represents the sampled received signal at the receiver RF block output.)

## Considerations for a CSK Modulation on a GNSS Receiver

Two of the major drawbacks of a CSK-modulated signal are the need for a pilot signal for synchronization purposes and the increase of the receiver complexity. In this section these issues are tackled through a comparison between the effects of CSK- and BPSK-modulated signals on a GNSS receiver. Except for the data-signaling scheme, the CSK and BPSK signals share similar properties and parameters:

- The total power of both signals is equally shared between a data and a pilot component.
- They have the same PRN chipping rate and the same primary PRN code length, both on data and pilot components.

**Impact on the Receiver Architecture.** The demodulation process of a CSK-modulated signal is intuitively more complex than the demodulation process of a BPSK modulation, because it requires more correlators. We assess the increase in complexity here by means of the number of multiplications required for the demodulation of both CSK and BPSK signals.
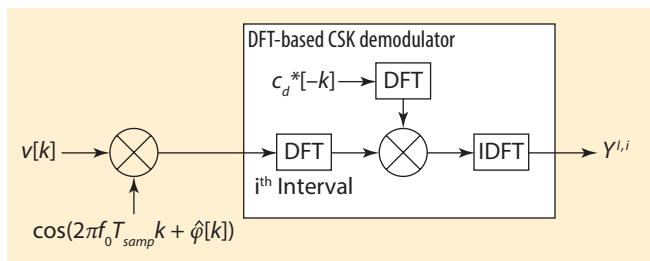


| | | Number of Multiplications | | |
|---|---|---|---|---|
| | | CSK | | BPSK |
| PRN Code Length | U | Radix-2 | Bank of Traditional Correlation | Correlator |
| 1023 | 6 | 11264 | 65472 | 6138 |
| | 8 | 11264 | 261888 | 8184 |
| 10230 | 6 | 245760 | 654720 | 61380 |
| | 8 | 245760 | 2618880 | 81840 |
| | 10 | 245760 | 10475520 | 102300 |
| | 12 | 245760 | 41902080 | 122760 |

**Table 1** Number of multiplications required for demodulating U bits/symbols with a *CSK(U,1)* configuration and a BPSK configuration  (from A. Garcia-Pena *et alia,* 2013)

**Table 1** shows the number of multiplications required when demodulating one symbol for a *CSK(U,1)* (mapping *U* bits and spanning *N*=1 PRN code) and for a traditional BPSK demodulator when *U* bits are sequentially demodulated.

Two types of demodulators are proposed for the CSK signal: a bank of matched filters (or correlators) and an FFT-based correlator with the radix-2 Cooley-Tukey FFT algorithm (described in the article by P. Marti-Puig). Although the FFT-based demodulator moderately reduces the complexity of a bank of matched filters demodulator, its complexity remains significantly higher than the complexity of a typical BPSK demodulator.

**Effect on Signal Acquisition.** Here we compare the joint data/pilot acquisition method (not applicable to CSK) and the pilot-only acquisition method (applicable to both modulations) in order to inspect the degradation on the acquisition sensitivity introduced by a CSK modulation on the data component. Both methods have the same frequency and code delay uncertainty, and use the same acquisition detector: the standard single dwell acquisition technique described by E. Kaplan and C. Hegarty (see Additional Resources).

**Table 2** and **Table 3** show the acquisition threshold (total signal $C/N_0$) for the joint data/pilot acquisition method and for the pilot-only acquisition method with different data/pilot power share and for different PRN code lengths, respectively, 1,023 and 10,230 chips. The targeted *false alarm probability* equals the inverse of the PRN length (~ $10^{-3}$ and $10^{-4}$) and the targeted *detection probability* is set to 90 percent. From these tables, we conclude that the BPSK modulation seems more appropriate for acquisition purposes, as it enables the possibility of a joint data/pilot acquisition. However, if a 75–25 percent pilot/data power split is used, BPSK and CSK signals would have similar performances.

**Effect on Signal Tracking.** The benefits of a pilot component in GNSS signal code and phase tracking have been widely demonstrated and publicized since the early 2000s. As reflected in the discussion in the works by E. Kaplan and C. Hegarty, and O. Julien, when the pilot component's power expressed relative to the composite data plus pilot signal's power is 50 percent or more, one may expect that most receivers will only rely on the



DFT-based CSK demodulator

$v[k]$ → ⊗ → DFT → ⊗ → IDFT → $Y^{l,i}$
$i^{th}$ Interval

$c_d{}^*[-k]$ → DFT

$\cos(2\pi f_0 T_{samp} k + \hat{\varphi}[k])$

**FIGURE 6** DFT-based CSK demodulator scheme

| Coherent Integration time (ms) | Dwell Time on 1 acquisition bin (ms) | Acquisition Technique (dB-Hz) | | |
|---|---|---|---|---|
| | | Pilot- or Data-only with 75% | Pilot- or Data-only with 50% | Data+Pilot |
| 1 | 10 | 34.7 | 36.4 | 34.4 |
| | 100 | 28.5 | 30.2 | 28.5 |
| | 500 | 24.6 | 26.3 | 24.7 |
| 10 | 10 | 32.1 | 33.8 | 31.5 |
| | 100 | 24.7 | 26.4 | 24.4 |
| | 500 | 20.3 | 22 | 20.2 |

**Table 2** Example of expected acquisition thresholds (Total Data+Pilot $C/N_0$ of the Signal) for PRN length of 1023 chips (from A. Garcia-Pena *et alia,* 2013)

| Coherent Integration time (ms) | Dwell Time on 1 acquisition bin (ms) | Acquisition Technique (dB-Hz) | | |
|---|---|---|---|---|
| | | Pilot- or Data-only with 75% | Pilot- or Data-only with 50% | Data+Pilot |
| 1 | 10 | 35.3 | 37 | 35.2 |
| | 100 | 29.2 | 30.9 | 29.1 |
| | 500 | 25.2 | 26.9 | 25.3 |
| 10 | 10 | 33.1 | 34.8 | 32.4 |
| | 100 | 25.5 | 27.2 | 25.2 |
| | 500 | 20.9 | 22.7 | 20.9 |

**Table 3** Example of expected acquisition thresholds (Total Data+Pilot $C/N_0$ of the Signal) for PRN length of 10230 chips (A. Garcia-Pena *et alia,* 2013)

pilot component for tracking in order to benefit from:

- larger coherent integration time on both code and carrier tracking (phase and/or frequency) and
- more robust and more linear discriminator or estimator for the carrier tracking (phase and/or frequency).

In this case the data component will be processed only for demodulation purposes.

A consequence of these assumptions is that we should expect the CSK implementation on the data component to have limited effects on the receiver's tracking performance as long as enough power is allocated to the pilot component.

## Bit Error Corrections Schemes Adapted to CSK Modulations

The robustness against errors of a digital message defined by a sequence of information bits, is usually characterized by the bit error rate (BER) and the associated metrics such as *word*, *page*, or *frame error rate*. In the case of a navigation message containing the ephemeris and clock data necessary to compute the PVT solution, we also introduced the *CED error rate* in order to define the robustness of message reception.

The error rate metric is a function of the $E_b/N_0$, translating the ratio between the energy carried by an information bit and the noise power density. Rather than increasing the effective $E_b/N_0$ by reducing the bit rate or by increasing the received power in order to improve the message reception's robustness to errors, an efficient approach is to rely on error correction codes, also known as channel codes.

The application of a channel code consists of introducing —in a controlled manner — redundant bits into the message. By exploiting this redundancy the receiver is able to correct some errors introduced by the channel. This channel code decreases the demodulation threshold and increases the signal data availability.

Although the first civil GNSS signals, GPS and GLONASS C/A, do not implement a channel code specifically dedicated to error correction, all modernized signals possess one. The most classical scheme relies on binary channel codes, of which the most well-known in the GNSS field is the standard Consultative Committee for Space Data Systems (CCSDS) convolutional code (7, ½), used in Galileo signals, as well as in GPS L2C, L5, and SBAS signals.

The newest GNSS signals are protected by more powerful channel codes, such as the low density parity check (LDPC) used in the GPS III civil signal, L1C, or the Reed-Solomon (Non-binary or Q-ary) codes. Although common in satellite communications (e.g., Reed-Solomon is used for DVB-S channel code), these latter options are not often used currently in GNSS. We can cite as an example the QXSS LEX signal.

Note that the correction capacity of the channel code will also depend on the chosen decoding method within the receiver. Many pairs of encoding processes and decoding schemes may be proposed for a CSK signal. In this article, we identify several examples and describe them further in the following sections.

### Two Examples of Encoding Schemes
**Binary Channel Codes.** In this case, the channel code implemented in the latest designed GNSS signal, the rate ½ LDPC channel code of the GPS L1C subframe 2, has been used with a CSK-modulated signal, in order to compare the CSK with the BPSK modulation results.

Following the encoding process, two different methods (presented schematically in **Figure 7**) have been applied to sort and map the encoded bits into CSK symbols, referred to as mapping A or mapping B and defined in the papers by A. Garcia-Pena *et alia*, 2010 and 2013. Mapping B directly maps the encoded bits in their temporal order, and thus all the bits mapped by a CSK symbol belong to the same message. Mapping A consists of mixing the encoded bits through an interleaver and, as a result, each bit mapped by a CSK symbol is forced to belong to a different message.

**Non–Binary Channel Codes.** In a Q-ary channel code, each channel code symbol maps a determined set of Q bits. Therefore, the typical design of a Q-ary channel code on a CSK signal consists of having the same size (or number of bits) for a Q-ary symbol as for a CSK symbol
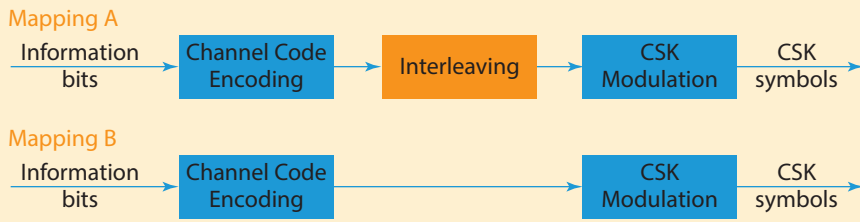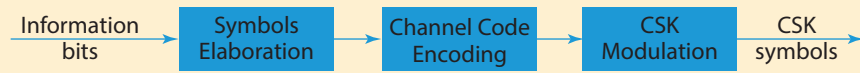
**FIGURE 7** CSK codeword source mappings A and B



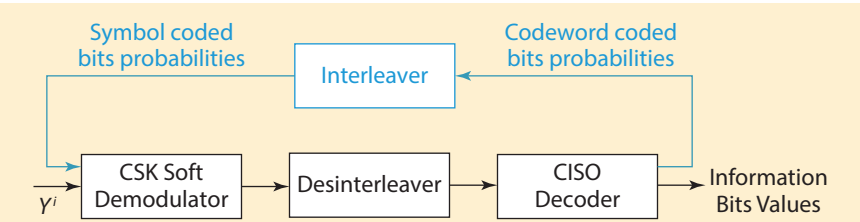**FIGURE 8** CSK codeword source mappings for a non-binary channel code



**FIGURE 9** CSK sequential and iterative decoding method

| | Channel Code | Decoding Algorithm | Propagation Channel | Mapping | Encoded Bit Rate (symbol rate) of the various CSK configurations (bps) |
|---|---|---|---|---|---|
| Figure 10 | Binary: GPS L1C subframe 2 rate ½ LDPC | Sequential and Iterative | AWGN | B | 500, 1000, 1500,2000, 2500 and 2750 |
| Figure 11 | | | | A | 500, 1000, 1500, 2000 and 2750 |
| Figure 12 | | | | B | 250 |
| Figure 13 | | | LMS channel: Perez-Fontan model | B | 500 |
| Figure 14 | | | | A | 500 |
| Figure 15 | Non binary: rate ½ Reed-Solomon | Sequential | AWGN | --- | 500, 1000 and 1250 |

**Table 4** Simulations parameters summary

($U = Q$). In doing so, each Q-ary symbol may be directly transmitted by one CSK symbol since they represent the same set of Q bits (see **Figure 8**).

In this case, the family of channel codes implemented in the QZSS-LEX signal, primitive Reed-Solomon channel codes, has been used with a CSK signal. But in order to be able to provide a straight forward comparison between binary (rate ½ LDPC) and non-binary channel codes schemes, the Reed-Solomon code rate has been forced to ½

(which is different from the QZSS LEX Reed-Solomon rate).

**Two Examples of Decoding Schemes.** At receiver level, the decoding algorithms may be sorted into two main groups: sequential decoding algorithms (direct classical technique) or iterative decoding algorithms as shown in **Figure 9**:

• Sequential algorithm: the decoder's outputs are considered to be the information bits estimated by the receiver, and as such, are sent to any downstream processing block (for

example, CRC). It is easy to apply, and requires limited memory (A. Garcia-Pena *et alia,* 2013).

• Iterative algorithm, for example the bit-interleaved coded modulation with iterative decoding (BICM-ID) (described in G. Caire *et alia*): the output of the decoder is fed back into the demodulator/decoder to refine the bit estimation. This feedback may be repeated several times before the decoder decides to output the final information bits. The performance, along with the processing power and memory required, increase with the number of iterations.

In case an interleaver is applied at the emitter level, the receiver must implement a disinterleaver for both the sequential and iterative algorithms, and also the associated interleaver for the iterative algorithm (see Figure 9).

## Examples of Demodulation Performance of Correction Schemes

This section presents the results of some demodulation performance simulations, comparing the bit error rate (BER) versus the carrier-to-noise-density ($C/N_0$) for various CSK configurations, in the presence of average white Gaussian noise (AWGN) or LMS (land mobile satellite, urban environment) propagation channels.

The following assumptions are made in every analyzed case:

• The primary PRN code duration is Ts = 4 milliseconds, which yields a bit rate of 250 encoded bits per second, for a BPSK modulation where one PRN code spans one encoded bit or BPSK symbol.

• The $C/N_0$ provided in all the figures refers to the data component $C/N_0$ only.

• For both propagation channels (AWGN, LMS), perfect code delay and carrier frequency estimation are assumed, as well as a perfect frame or page synchronization and the noise power is assumed to be perfectly known.

• For simulations in an AWGN channel, a coherent demodulation is conducted and a perfect carrier phase
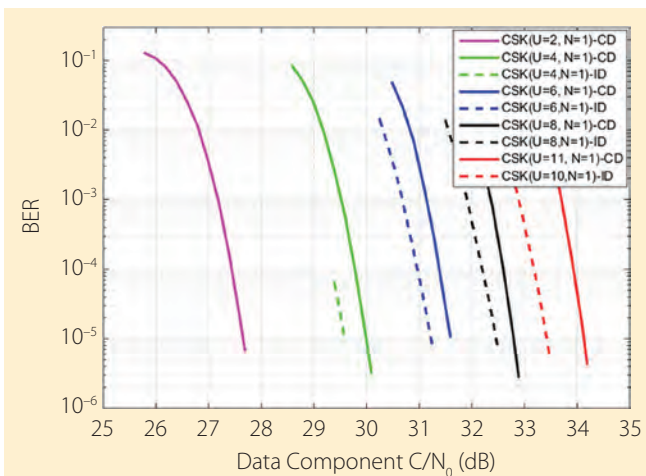
**FIGURE 10** BER vs C/N₀ of a CSK signal using the "mapping B" encoding process in an AWGN channel
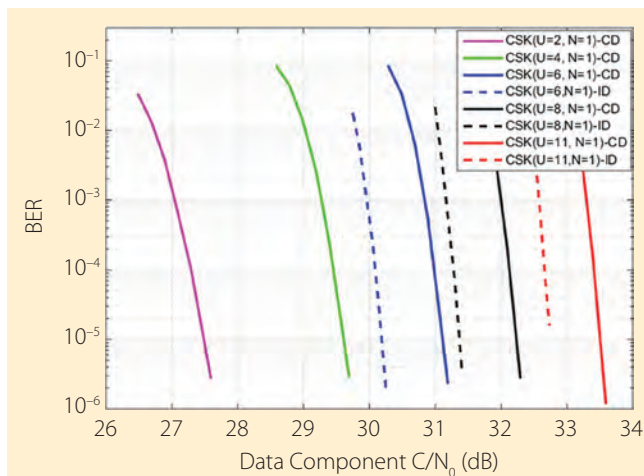


**FIGURE 11** BER vs C/N₀ of a CSK signal using the "mapping A" encoding process in an AWGN channel



**FIGURE 12** BER vs C/N₀ of different CSK configurations with "mapping B" having the same bit rate in an AWGN channel

estimations is assumed.

- For simulations in a LMS channel, a non-coherent demodulation is conducted and the channel attenuation impact $a(t)$ is assumed to be perfectly known.
- The chosen LDPC decoding method to be implemented in the SISO decoder (see Figure 9) is the classical message-passing or propagation-belief algorithm (see F. R. Kschischang *et alia*).
- The chosen Reed-Solomon decoding method to be implemented in the decoder block (Figure 9) is the Berlekamp/Forney algorithm (described in the article by S. Lin *et alia*). Note that the bit rate presented in **Table 4** corresponds to the bit rate of the coded bits (sometimes also referred to as symbols). In order to obtain the useful information bit rate, Table IV rates must be multiplied by the channel code rate, equal to ½.

## Binary Channel Code Correction Schemes in AWGN Channel

**Figure 10** and **Figure 11** show the C/N0 required to obtain a given BER (usually a value of 10-5 is targeted) when the bit rate is increased by a factor of $U$ with respect to BPSK-modulated signal with one symbol or encoded bit = one PRN code (250 sps for $T_s$ = 4 ms). From those two figures, we can see that mapping A outperforms mapping B and that iterative decoding also outperforms classical decoding.

**Figure 12** shows various CSK configurations, all providing the same encoded bit rate of 250 bps. These configurations are benchmarked to a 250 bps BPSK modulation with LDPC encoding (information bit rate of 125 bps). Mapping B configurations are the only ones selected, because they generate messages with a time duration (or latency) equal to the benchmarked BPSK signal and thus yield a fair comparison between the different options.

From Figure 12, we observed that the demodulation performance improves when more bits are mapped on a CSK symbol. However, this also implies potential limitations, as the CSK symbol must be longer to obtain the same bit rate. Moreover,
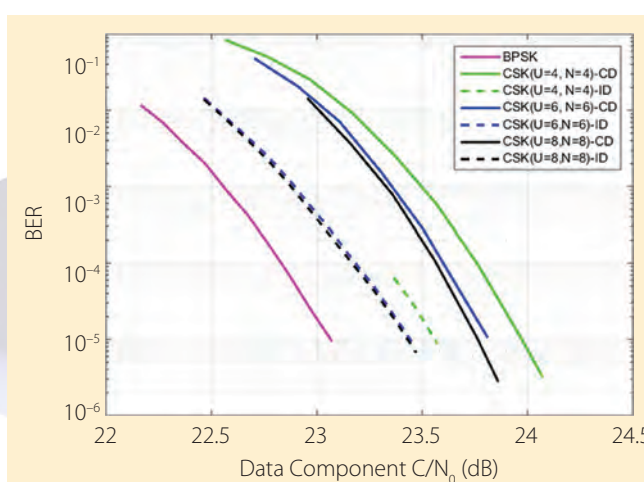
this improvement seems to reach a saturation point when a certain number of bits mapped by a CSK symbol is attained.

Finally, current CSK configurations with GPS L1C subframe 2 rate ½ LDPC channel code, mapping B, and the same message time duration (or latency) are still outperformed by a classical BPSK-modulated signal. As the selected LDPC was specially designed to be implemented in a BPSK modulation and not in a CSK modulation, it is expected that this degradation could be mitigated (and the effect even inversed) by specifically designing channel codes adapted to CSK, as investigated by M. Aubault-Roudier *et alia*.

## Binary Channel Code Correction Schemes in an Urban Environment for a Non-Coherent Demodulation Process

The simulated urban environment represents an LMS channel, based on the Perez-Fontan channel mathematical model. This channel model characterizes the $c(t)$ values with a Loo distribution, as described in the articles by F. Perez-Fontan *et alia*) and (R. Prieto-Cerdeira *et alia*) and is assumed to be non-frequency
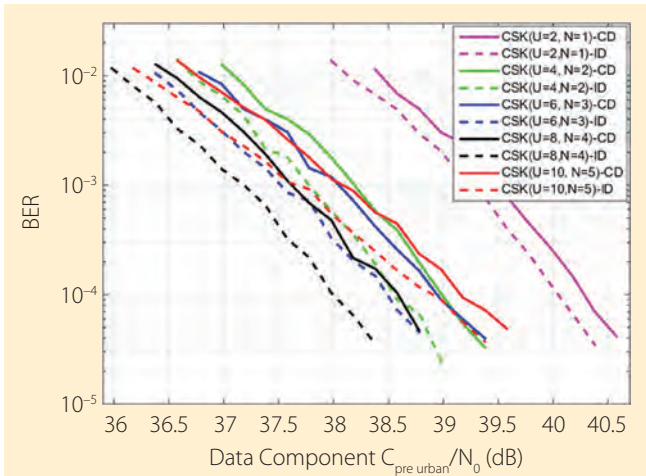
**FIGURE 13** Bit error rate versus carrier-to-noise-density ratio of a CSK signal using the "mapping B" encoding process with twice the BPSK signal bit rate in an LMS channel
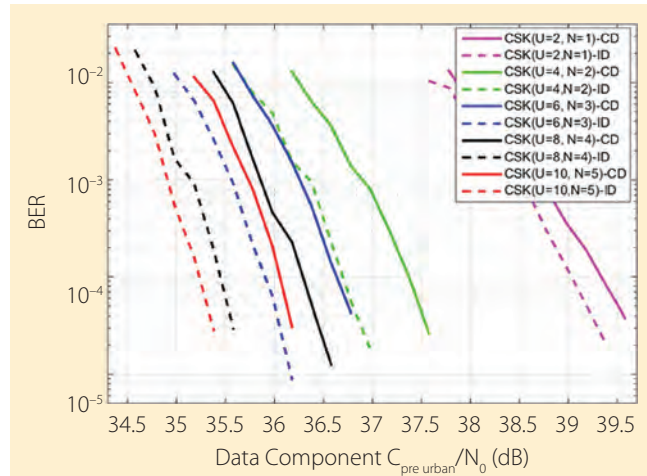


**FIGURE 14** Bit error rate versus carrier-to-noise-density ratio of a CSK signal using the "mapping A" encoding process with twice the BPSK signal bit rate in an LMS channel
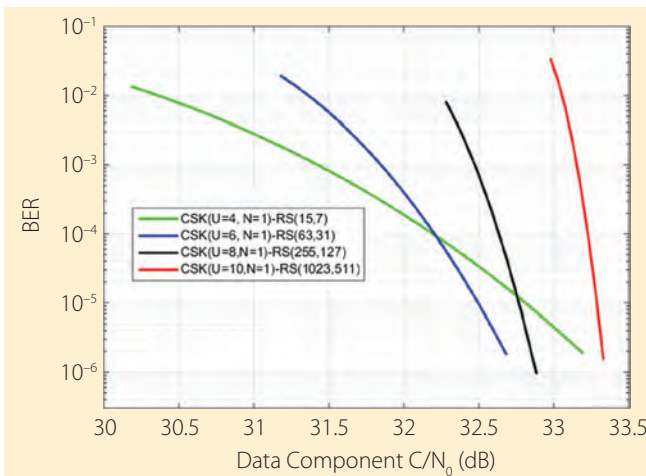


**FIGURE 15** Bit error rate versus carrier-to-noise-density ratio of a CSK signal with a Reed-Solomon channel code with r=1/2 in an AWGN channel

selective, and thus the received signal can be modeled as presented in Equation (5).

Only the "intermediate shadowing" state of the Perez-Fontan model is simulated with the following loop parameter values, $\alpha = -8dB$, $\Psi = 4.5dB$, MP = -19,2dB, because this state is representative of moderate-to-difficult reception conditions. The user speed is set to 50 km/h and the satellite elevation angle to 40 degrees. We have used the non-coherent demodulation process described in the paper by A. Garcia-Pena *et alia* (2014)).

$C_{pre\_urban}/N_0$ is defined as the useful signal power at the correlator output when the propagation channel impact is not taken into account (except for space free losses). **Figure 13** and **Figure 14** show the BER as a function of the data component $C_{pre\_urban}/N_0$ of a CSK signal with a bit rate increase equal to two with respect to the BPSK signal (with one symbol = one PRN code) when conducting a non-coherent demodulation.

From Figure 13 and Figure 14, one can observe that the combination of a CSK signal and a non-coherent demodulation process eases transmission of information through environments

with moderate/difficult reception conditions. An important outcome of those results is that the best demodulation performances are no longer obtained by CSK configurations that map a lot of bits per symbol (A. Garcia-Pena *et alia*, 2010a). Long CSK symbol duration appears to be detrimental in urban environments (Figure 13 with "mapping B").

## Q-ary Channel Code Correction Scheme in AWGN Channel

We also performed a simulation of a CSK signal encoded by the non-binary rate ½ Reed-Solomon channel code and tested in an AWGN propagation channel. Figure 15 presents the results of the BER versus the data component $C/N_0$ for different CSK configurations *CSK(U,1)*.

**Figure 15** indicates that, for a CSK modulation, a Reed-Solomon channel code with a low number of bits mapped by a Q-ary (or CSK) symbol is suboptimal. In fact, when compared to binary channel code correction schemes, it appears that at least eight bits should be mapped in order to obtain the full potential of the Reed-Solomon scheme, although in such cases, the message duration becomes large.

## Conclusions

This article has presented the CSK modulation principle, highlighting some of its specific features related to demodulation performance.

We identified various correction schemes for CSK, using either binary channel code (binary LDPC) with classical or iterative decoding, or Q-ary channel code (Reed-Solomon). The results show that CSK is very sensitive to appropriate channel code design. However, this analysis still needs further refinement, as the binary channel code tested in this article is the GPS L1C subframe 2 LDPC code, which was specially designed for a BPSK modulation and not for a CSK modulation.

Over AWGN propagation channels, the results contributed to confirmation of the expected behavior of the CSK encoding as an *M*-ary signaling technology. CSK provides interest-

ing demodulation properties but does not outperform BPSK implementation with equivalent bit rates and with the same message time duration or latency (at least for the cases presented in this study).

Over LMS propagation channels, the results obtained thus far are encouraging. We would expect that, thanks to appropriate channel encoding, equalization, and non-coherent Rake-like receiver implementation, the CSK modulation could improve data availability in urban canyons.

Nevertheless, in comparison with a BPSK modulation, CSK modulation also has some drawbacks:

- First, the complexity of the receiver is significantly increased. Although efficient CSK-demodulation schemes in the frequency domain would moderately reduce the complexity, they remain generally more complex than the traditional BPSK demodulator.
- Second, the signal synchronization can no longer be conducted over the data component, and thus a pilot component is mandatory. As most modernized GNSS signals already rely on a pilot component, this drawback has limited impact, except perhaps on acquisition sensitivity.

All of this motivates additional work on CSK. Ongoing work aims at the optimization of the encoding-decoding

Results show that CSK is **very sensitive** to appropriate channel code design. However, this analysis still **needs further refinement…**

scheme, combined with appropriate channel equalization, non-coherent demodulation, and Rake-like receiver architecture, with the objective of achieving optimal performance in urban environments and finalizing our understanding and assessment of CSK's pros and cons. Further results are expected in the upcoming months, which should provide opportunities to consolidate the lessons learned about the CSK potential for GNSS signals.

## Additional Resources

**[1]** Caire, G., and G. Taricco, and E. Biglieri, "Bit-Interleaved Coded Modulation," *Proceedings of the IEEE International Symposium on Information Theory,* 29 June - 4 July 1997

**[2]** Dillard, G. M, and M. Reuter, J. Zeiddler, and B. Zeidler, "Cyclic Code Shift Keying: A Low Probability of Intercept Communication Technique," *IEEE Transactions on Aerospace and Electronic Systems,* Vol. 39, No 3, July 2003

**[3]** Garcia-Pena, A. (2014), and P. Paimblanc, O. Julien, L. Ries, and T. Grelier, "Analysis of Different CSK Configurations in an Urban Environment When Using Non-coherent Demodulation," *7th ESA Workshop on Satellite Navigation Technologies and European Workshop on GNSS Signals and Signal Processing* (NAVITEC), December 3–5, 2014

**[4]** Garcia-Pena, A. (2010), and M-L. Boucheret, C. Macabiau, J-L. Damidaux, L. Ries, Stéphane Corazza, and A-C. Escher, "Implementation of Code Shift Keying Signalling Technique in GALILEO E1 Signal," *5th ESA Workshop on Satellite Navigation Technologies and European Workshop on GNSS Signals and Signal Processing* (NAVITEC), December 8–10, 2010

**[5]** Garcia-Pena, A. (2013), and D. Salos, O. Julien, L. Ries, and T. Grelier, "Analysis of the Use of CSK for Future GNSS Signals," *Proceedings ION GNSS 2013+,* Nashville Tennessee USA, September 16–20, 2013

**[6]** Japan Aerospace Exploration Agency, I*nterface Specification for QZSS (IS-QZSS) Draft V1.6,* November 28, 2014

**[7]** Julien, O., *Design of Galileo L1F Receiver Tracking Loops,* Ph.D. Thesis, Department of Geomatics Engineering, University of Calgary, Canada, July 2005

**[8]** Kaplan, E. and Hegarty, C., *Understanding GPS: Principles And Applications,* Artech House, 2005

**[9]** Kschischang, F. R., and B. Frey, and H.-A. Loeliger,, "Factor Graphs and the Sum-Product Algorithm," *IEEE Transactions on Information Theory,* Vol 47, Issue 2, pages 498-519, February 2001

**[10]** Lin, S. and D.J. Costello, *Error Control Coding: Fundamentals and Applications,* second edition, Pearson – Prentice Hall, 2004

**[11]** Marti-Puig, P., "Two Families of Radix-2 FFT Algorithms With Ordered Input and Output Data," *IEEE Signal Processing Letters,* Vol. 16, Issue 2, pages 65–68, February 2009

**[12]** Perez-Fontan, F., and M. A. Vázquez-Castro, S. Buonomo, J. P. Poiares-Baptista, and B. Arbesser-Rastburg, B, ,"S-Band LMS Propagation Channel Behaviour for Different Environments, Degrees of Shadowing, and Elevation Angles, *IEEE Transactions on Broadcasting,* Vol. 44, No. 1, March 1998

**[13]** Prieto-Cerdeira, R., and F. Schubert, R. Orus-Perez, J.A. Garcia-Molina, and F. Zanier, "Flexible Statistical Multipath and Shadowing Model for Software and Hardware Simulations, *Proceedings ION GNSS+ 2011,* Portland, Oregon, USA 2011

**[14]** Proakis, J. G. and Salehi, M., *Digital Communications,* 5th ed, McGraw-Hill, 2008

**[15]** Roudier, M., and A. Garcia-Pena, O. Julien, T. Grelier, L. Ries, C. Poulliat, M-L. Boucheret, and D. Kubrak, "Demodulation Performance Assessment of New GNSS Signals in Urban Environments," *Proceedings ION GNSS+ 2014,* Tampa, Florida USA September 8–12, 2014

**[16]** Wong, A. Y.-C. and V. C. M. Leung, V. C. M., "Code-Phase-Shift Keying: A Power and Bandwidth Efficient Spread Spectrum Signaling Technique for Wireless Local Area Network Applications," *IEEE Canadian Conference on Electrical and Computer Engineering,* 1997

## Authors

**Axel Garcia-Peña** is a researcher/lecturer with the SIGnal processing and NAVigation (SIGNAV) research group of the TELECOM lab of École Nationale de l'Aviation Civile (ENAC, French Civil Aviation University), Toulouse, France. He received his double engineer degree in digital communications from SUPAERO and UPC, and his Ph.D. from the Department of Mathematics, Computer Science and Telecommunications of the INPT (Polytechnic National Institute of Toulouse), France.His research interests are GNSS navigation message demodulation, optimization and design, GNSS receiver design, and GNSS satellite payload.

**Marion Aubault-Roudier** is a radionavigation engineer in the navigation/location signals department in CNES, the French Space Agency, where she is involved in the optimization of GNSS signals as wells as the assessment of GNSS user segments (receivers, algorithms). Roudier graduated as an electronics engineer from ENAC (Ecole Nationale de l'Aviation Civile) in Toulouse, France. She received her Ph.D. from the Department of Mathematics, Computer Science and Telecommunications of the INPT (Polytechnic National Institute of Toulouse), France.

**Marie-Laure Boucheret** received the electrical engineering degree from ENST Bretagne and a Ph.D. degree in communications from TELECOM ParisTech. She has been a successful research engineer at the French Philips Research Laboratory (1985¬–1986), engineer at Thales Alenia Space in telecommunication and transmission (1986–1991), associated professor then a Professor at TELECOM ParisTech (1991–2005). Since 2005, Boucheret has been a Professor at the National Polytechnic Institute of Toulouse (ENSEEIHT - University of Toulouse). She is also with the Signal and Communication group of the IRIT Laboratory. Her main research interests include design of modulation and coding schemes for satellite communications, and algorithms and architecture of digital receivers.

**Charly Poulliat** received an electrical engineering degree from ENSEA, Cergy-Pontoise, France, an M.Sc. degree in signal and image processing from the University of Cergy-Pontoise and his Ph.D. degree in signal processing for digital communications from the University of Cergy-Pontoise. Since 2011, Poulliat has been a professor with the National Polytechnic Institute of Toulouse (ENSEEIHT - University of Toulouse). He has been the head of the Signal and Communications Group of the IRIT Laboratory since 2013. His main research interests include: signal processing for digital communications (satellite and terrestrial), analysis, design and optimization of iterative receivers, andchannel coding (LDPC codes, turbo codes) and related iterative decoders.

**Olivier Julien** is the head of the SIGnal processing and NAVigation (SIGNAV) research group of the TELECOM lab of ENAC (Ecole Nationale de l'Aviation Civile), Toulouse, France. He graduated as an electrical engineer from the ENAC and received his Ph.D. from the Department of Geomatics Engineering at the University of Calgary, Canada. Julien's research interests are GNSS receiver design, GNSS multipath and interference mitigation, and GNSS interoperability.

**Lionel Ries** is head of the navigation/location signals department in CNES, the French Space Agency. The department activities cover signal design and processing, receivers and payloads regarding location and navigation systems including GNSS (Galileo, GNSS space receivers), Search & Rescue by satellite (SARSAT, MEOSAR), and Argos (Advanced Data Collection and Location by Satellite, mostly for environment and wildlife monitoring). He also coordinates CNES research activities for future location/navigation signals, user segments equipment, and payloads.

**Prof.-Dr. Günter Hein** serves as the editor of the Working Papers column. He served as the head of the EGNOS and GNSS Evolution Program Department of the European Space Agency and continues to advise on scientific aspects of the Navigation Directorate as well as being a member the ESA Overall High Level Science Advisory Board. Previously, he was a full professor and director of the Institute of Geodesy and Navigation at the Universität der Bundeswehr München (UniBW), where he is now an ""Emeritus of Excellence." In 2002, he received the Johannes Kepler Award from the U.S. Institute of Navigation (ION). He is one of the inventors of the CBOC signal. **IG**